

Evidence of in vivo exogen protein uptake by red blood cells: a putative therapeutic concept

Laura Hertz,¹ Daniel Flormann,² Lutz Birnbaumer,^{3,4} Christian Wagner,^{2,5} Matthias W. Laschke,⁶ and Lars Kaestner^{1,2}

¹Theoretical Medicine and Biosciences, Medical Faculty, Saarland University, Homburg, Germany; ²Dynamics of Fluids, Experimental Physics, Saarland University, Saarbruecken, Germany; ³Institute of Biomedical Research (BIOMED), Catholic University of Argentina, Buenos Aires, Argentina; ⁴Laboratory of Signal Transduction, National Institute of Environmental Health Sciences, Research Triangle Park, NC; ⁵Physics and Materials Science Research Unit, University of Luxembourg, Luxembourg City, Luxembourg; and ⁶Medical Faculty, Institute for Clinical and Experimental Surgery, Saarland University, Homburg, Germany

Key Points

- Transfusion of TRPC6 knockout RBCs to wild-type mice led to the “rescue” of TRPC6 function, suggesting protein transfer to RBCs.
- Mechanical stimulation leads to tether formation between human RBCs, which may mediate protein transfer, a key for a new treatment concept.

For some molecular players in red blood cells (RBCs), the functional indications and molecular evidence are discrepant. One such protein is transient receptor potential channel of canonical subfamily, member 6 (TRPC6). Transcriptome analysis of reticulocytes revealed the presence of TRPC6 in mouse RBCs and its absence in human RBCs. We transfused TRPC6 knockout RBCs into wild-type mice and performed functional tests. We observed the “rescue” of TRPC6 within 10 days; however, the “rescue” was slower in splenectomized mice. The latter finding led us to mimic the mechanical challenge with the cantilever of an atomic force microscope and simultaneously carry out imaging by confocal (3D) microscopy. We observed the strong interaction of RBCs with the opposed surface at around 200 pN and the formation of tethers. The results of both the transfusion experiments and the atomic force spectroscopy suggest mechanically stimulated protein transfer to RBCs as a protein source in the absence of the translational machinery. This protein transfer mechanism has the potential to be utilized in therapeutic contexts, especially for hereditary diseases involving RBCs, such as hereditary xerocytosis or Gárdos channelopathy.

Introduction

The molecular signaling capacity of red blood cells (RBCs) is increasingly recognized¹⁻³ as is their functional heterogeneity.^{4,5} In this context, ion channels are also slowly being acknowledged as physiologically relevant signal mediators in RBCs^{6,7} although their copy number per cell is very low.⁸⁻¹⁰

The presence of transient receptor potential channel of canonical type, member 6 (TRPC6) has been indicated in the protein level in mature RBCs,¹¹ but this finding was controversially discussed. Direct pharmacological agents (agonists and antagonists) for TRPC6 are limited, and inhibitors are not effective against RBCs.¹²

Expelling the nucleus and all other organelles during erythropoiesis leaves the RBCs without a translational machinery for an average of 120 days (in humans) without protein (including ion channel) renewal or any other repair mechanism.¹³

Submitted 22 June 2022; accepted 20 November 2022; prepublished online on *Blood Advances* First Edition 9 December 2022; final version published online 20 March 2023. <https://doi.org/10.1182/bloodadvances.2022008404>.

Data are available on request from the corresponding author, Lars Kaestner (lars_kaestner@me.com).

The full-text version of this article contains a data supplement.

© 2023 by The American Society of Hematology. Licensed under [Creative Commons Attribution-NonCommercial-NoDerivatives 4.0 International \(CC BY-NC-ND 4.0\)](https://creativecommons.org/licenses/by-nc-nd/4.0/), permitting only noncommercial, nonderivative use with attribution. All other rights reserved.

Methods

Blood was taken from healthy volunteers with informed consent; the protocol was in agreement with the Declaration of Helsinki and authorized by the ethics committee of the Ärztekammer des Saarlandes (permission number 132/08). Mouse experiments were approved by the respective commission of the Saarland (permits 02/2015 and 27/2018).

Transcriptome analysis

Transcriptome analysis was performed as previously described.¹⁴ In short, to purify human RBCs we followed a method originally developed by Beutler et al.¹⁵ To evaluate the purification of the RBCs, we used the gelatin zymography technique, previously described by Achilli et al.¹⁶ This method allows the detection of contaminations with polymorphonuclear neutrophils, a type of leucocyte that cannot be eliminated by washing the blood sample. Polymorphonuclear neutrophils are the only type of blood cells that express the matrix metalloproteinase 9, whose catalytic activity against gelatin can be used as a specific marker.

Fluorescence-activated cell sorting was performed with wild-type (WT) murine blood samples using a FACSaria III (Becton Dickinson, Franklin Lakes, NJ).

For RNA isolation, we used the RiboPure RNA Purification Kit (Thermo Fisher Scientific, Waltham, MA) and 500 μ L of human or murine blood samples, prepared as described before. Subsequently, the α - and β -globin messenger RNAs, which have the highest expression in reticulocytes, were removed from the total RNA preparations by using the GLOBINclear Kit (Thermo Fisher Scientific) according to the manufacturer's protocol. Transcriptome analysis was performed by Expression Analysis Inc (Durham, NC) using next-generation sequencing. More information are detailed in the supplemental Material.

Ca²⁺ imaging

Life cell imaging was performed to monitor intracellular Ca²⁺ kinetics in individual cells stimulated with 5 μ M lysophosphatidic acid (LPA; Cayman Chemicals, Ann Arbor, MI). RBCs were washed 3 times with Tyrode solution (Tyrode) containing the following components: 135 mM NaCl, 5.4 mM KCl, 10 mM glucose, 1 mM MgCl₂, 1.8 mM CaCl₂, and 10 mM *N*-2-hydroxyethylpiperazine-*N*'-2-ethanesulfonic acid. The pH was adjusted to 7.35 using NaOH. For imaging, the cells were loaded with Fluo-4 (Fluo-4 AM; Molecular Probes, Eugene, OR) at a concentration of 5 μ M for 1 hour at 37°C. Then, the cells were washed 3 times with Tyrode. The Fluo-4-loaded cells were plated onto coverslips. We waited for 15 minutes for cell sedimentation and dye de-esterification. Fluorescence was measured on the stage of an inverted microscope (TE2000; Nikon, Tokyo, Japan) equipped with a 100 \times objective (CFI Plan Fluor 100 \times oil, numerical aperture = 1.3; Nikon). A video imaging device (TILL Photonics, Germany) was attached to the microscope and contained a monochromator (Polychrome V), a sCMOS camera (Flash4; Hamamatsu Photonics, Shizuoka, Japan), the imaging control unit, and an acquisition software (LightAcquisition; FEI, Munich, Germany). Fluo-4-loaded cells were excited at 480 nm and the resulting fluorescence images (using a 505 nm long pass dichroic mirror and a 535/40 bandpass filter) were collected every 5 seconds for 15 minutes. A gravity-driven local perfusion system was

utilized to quickly exchange solutions in the field of view. All measurements were performed at room temperature (\sim 22°C) and are represented in Figure 1A-B of the article and the corresponding image sequences are provided as supplemental Videos. These images were analyzed in ImageJ (Wayne Rasband, National Institutes of Health, Bethesda, MD), that is, individual cells were marked with regions of interest and background-corrected single mean intensity cell traces extracted over time. Because a real quantitative fluorescence-based Ca²⁺ measurement is still not possible as of now,¹⁷ the traces are plotted as a semiquantitative self-ratio of F/F_0 , with F being the recorded fluorescence intensity over time and F_0 being the fluorescence intensity at the start of the measurement (here, the average of the first 12 data points). Because the response is extremely heterogeneous, the analysis of the fluorescence intensity at a given time point is not representative and instead, for each trace the maximum intensity is determined⁴ utilizing custom-made macros in MATLAB (MathWorks, Natick, MA). This usually gives a not normalized distribution of Ca²⁺ intensity values. Thus, the median value for each mouse is then plotted in Figure 1C,E as 1 data point and is used in the statistics presented in Figure 1D,F.

Transfusion experiments

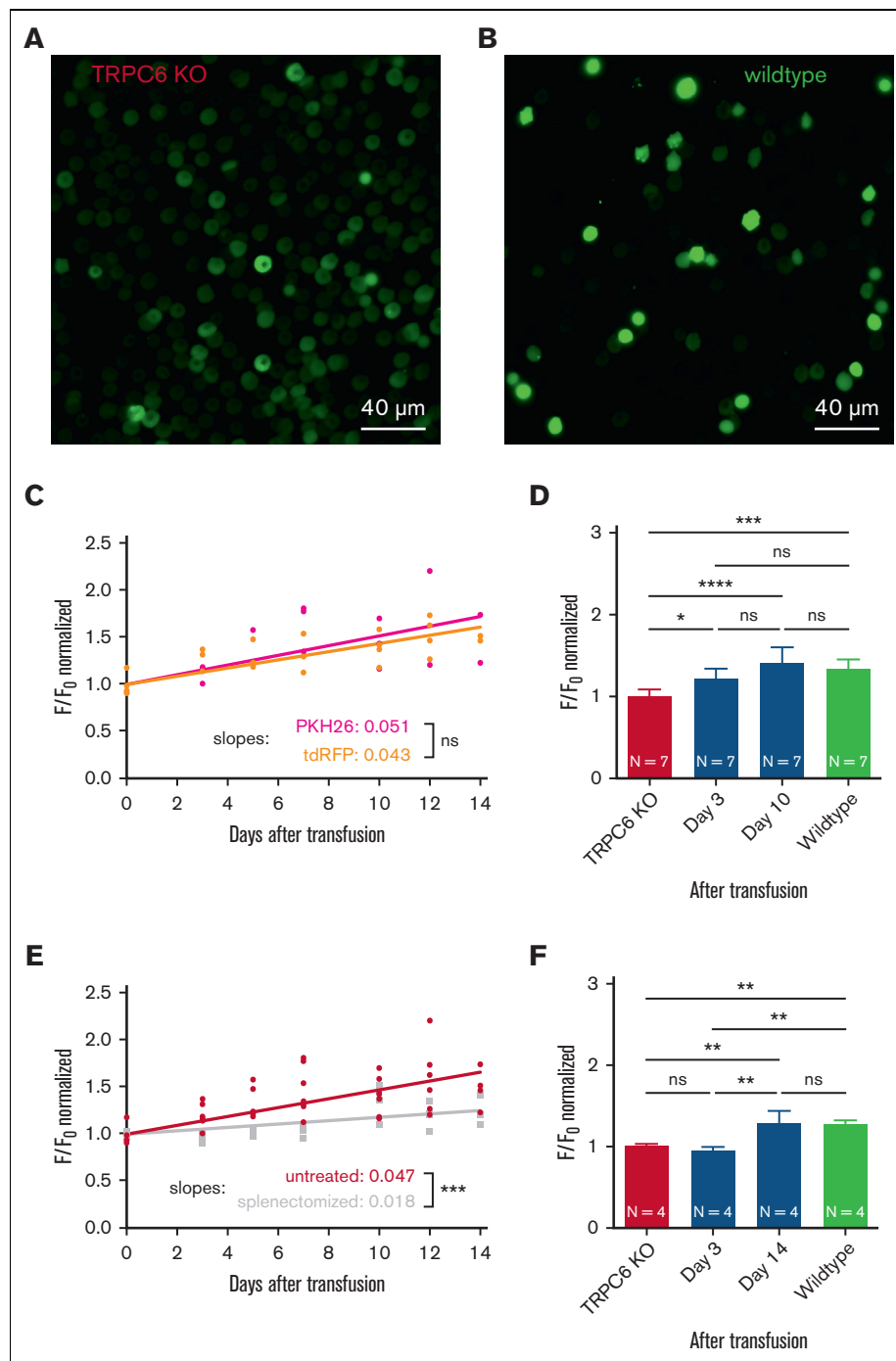
For transfusion experiments, blood was collected from TRPC6-knockout (KO) mice (average age of 17.5 ± 6.2 weeks, normal distributed) by puncture of the heart (final bleeding after 1.5% isoflurane inhalation anesthesia). RBCs (if not expressing the tandem-dimer red fluorescent protein [tdRFP]) were stained using the membrane dye PKH67 (Sigma-Aldrich, St Louis, MO). Cells were washed thrice in 0.9% NaCl solution and incubated for 5 minutes at room temperature under rotation with PKH26 (1:200 dilution). Quenching of remaining dye was done by addition of 2% bovine serum albumin in phosphate-buffered solution and the cells were washed again thrice in 0.9% NaCl solution. For transfusion, 200 μ L of stained or tdRFP-expressing TRPC6-KO RBCs were retro-orbitally injected into WT C57BL/6 mice (Charles River Laboratories, Senneville, Canada). We measured a RBC concentration of $9.2 \times 10^{12}/L$, resulting in $\sim 1.84 \times 10^9$ cells per transfusion. Recipient mice had an average age of 23.3 ± 10.9 weeks (normal distributed) and this did not significantly differ from that of the donor mice ($P = .26$). With the blood of 1 donor mouse, 2 to 3 WT mice could be transfused. The transfused RBCs were analyzed by Ca²⁺ imaging experiments, as described above, every 2 to 3 days for 2 weeks. For this purpose, a 10 μ L blood sample of each transfused mouse was collected by puncture of the facial vein.

Atomic force spectroscopy combined with confocal microscopy

All measurements were performed with the JPK Nanowizard 3 (Bruker, Berlin, Germany) setup coupled with a Nipkow-disk based confocal microscope. Before the measurements, RBCs were allowed to adhere to the microscope dish (microdish; Ibidi, Munich, Germany). Furthermore, RBCs were attached to the cantilever with Cell-Tak (Corning Inc, Corning, NY). Here the adsorption method was used, which can be described as follows: 10 μ L of Cell-Tak was mixed with 285 μ L of sodium bicarbonate (100 mM). The pH was adjusted to 8.0 using NaOH. The solution was appended to the substrate (cantilever). After a waiting time of

Figure 1. Transfusion of TRPC6-KO RBCs into WT mice.

(A) Microscopic fluorescence image of RBCs from a TRPC6-KO mouse loaded with the Ca^{2+} dye Fluo-4 (5 μM , 1 hour, 37°C) and immobilized with Cell-Tak). Microscopic imaging¹² was performed while the cells were stimulated with LPA (5 μM , 5 minutes). (B) Microscopic fluorescence image from the same experiment described in panel A but with RBCs from a WT mouse (C57Bl6/N). The full image sequences, where the images in panels A and B were taken from are provided in the supplemental Material. Scale bar, 40 μM (A-B). (C) Two hundred microliters of RBCs from total TRPC6-KO mice (hematocrit of 50% in a 0.9% NaCl solution) were transfused into WT mice (C57Bl6/N) by retrobulbar injection under isoflurane narcosis. First, TRPC6-KO RBCs were labeled with the dye PKH26 (Sigma-Aldrich)⁴ (dark red symbols). Alternatively, the TRPC6-KO mouse was crossbred with a mouse expressing tdRFP,¹⁹ that is, having RBCs with an intracellular fluorescent protein (light red symbols). Before transfusion and up to 14 days after transfusion, blood was sampled at the facial vein (10 μL) from the transfused mice. The relative number of PKH26/tdRFP-positive cells is provided in supplemental Figure 3A. RBCs were video imaged as shown in panels A and B for 15 minutes. The maximum value of the background-corrected, cellular F/F_0 signal of PKH26- or tdRFP-positive cells was analyzed.⁴ Each plotted data point is the median of at least 100 RBCs from 1 mouse (natural decrease in cell number over time after transfusion). (D) Replot of the data presented in panel C at selected time points and comparison to WT RBCs from the transfused mice. (E) Same experiments as in panel C with all data fitted together (red symbols) and similar experiments as in panel C but with WT mice splenectomized 1 week before transfusion (gray symbols). For splenectomy, mice were anesthetized by an injection of ketamine (75 mg/kg body weight) and xylazine (15 mg/kg body weight). After abdominal sectioning, the splenic vein and splenic artery were ligated, and the spleen was removed. The relative number of tdRFP-positive cells under the different experimental conditions is provided in supplemental Figure 3B. (F) Replot of the data presented in panel E at selected time points and comparison to WT RBCs from the transfused mice. In panels D and F, values are plotted as the mean \pm standard deviation. N, number of animals. In comparison, "ns" denotes not significant ($P \geq .05$), * $P < .05$, ** $P < .01$, *** $P < .001$, and **** $P < .0001$. Significance was tested with ordinary 1-way analysis of variance with Tukey multiple comparison tests (Prism 9, GraphPad Software, San Diego, CA).



at least 20 minutes, the cantilever was rinsed with distilled water and possibly phosphate-buffered saline.

A cell was "caught" with a setpoint force of 2.5 nN, a velocity of 5 $\mu\text{m/s}$ using a contact time of 10 seconds. While the cantilever was

in contact with the cell, it was moved by hand slightly ($\sim 2 \mu\text{m/s}$) in the x-y direction. When cells adhering to the microdish and cells attached to the cantilever were probed, force-distance curves were acquired with the following atomic force microscopy (AFM)-specific parameters: setpoint force, 300 pN; approach/retract velocity,

0.1 $\mu\text{m/s}$ with “breaks” for confocal imaging; and typical contact time, 30 seconds. The confocal scanning head was attached to an inverted microscope (Nikon Eclipse Ti; Nikon) equipped with a 60 \times objective (CFI Plan Achromat Lambda 60 \times oil, NA = 1.4; Nikon). A diode laser ($\lambda = 647 \text{ nm}$; Nikon LU-NV Laser Unit; Nikon) was used as a light source for imaging. Z-stack scanning was realized by employing a 100 nm piezo stepper. Confocal image generation was performed with a spinning-disk based confocal head (CSU-W1, Yokogawa Electric Corporation, Tokyo, Japan). Image sequences were acquired with a digital camera (Orca-Flash 4.0, Hamamatsu Photonics).

Results

In human reticulocytes (fluorescence-activated cell sorting for CD71⁺ and CD45⁻ cells), we could not find *TRPC6* (nor any other TRPC channel) (N = 4); whereas in mouse reticulocytes, we found the *TRPC6* transcript (GenBank BC068310), confirming the presence of TRPC6, which was also observed in western blots of mouse RBCs.^{11,18}

However, at the functional level, measured as LPA-induced Ca²⁺ entry,^{4,12} which was shown to involve TRPC6,¹² human and mouse WT RBCs give a similar Ca²⁺ response, but both differ from the Ca²⁺ response of TRPC6-KO mouse RBCs.¹²

The discrepancy between the lack of genetic proof of *TRPC6* and its putative functional presence in human RBCs suggested that TRPC6 is taken up by the RBCs from external sources. To test this hypothesis, we transfused fluorescently labeled RBCs^{4,19} from TRPC6 total KO mice into WT mice with the dye PKH26 used as a label.⁴ At different time points up to 2 weeks, we collected blood samples from the mice, performed LPA stimulation experiments, as shown in Figure 1A-B, and analyzed the PKH26-positive cells for their Ca²⁺ response (Figure 1C). This indirect method was used because the number of TRPC6 channels is expected to be below the detection limit of biochemical methods, such as western blotting and mass spectrometry. In addition, electrophysiological detection, for example, patch clamp recordings, is not an alternative because no direct activators of TRPC6 are available; hence, intracellular signaling is required for TRPC6 activation. (In the patch clamp configurations, the cytoplasm is normally washed out, except in the perforated-patch configuration, which is not available for RBCs.) Therefore, an amplification mechanism, such as the accumulation of Ca²⁺ inside the cell, seems to be the only available method for the detection of the TRPC6 channel activity in RBCs at present.

We performed such measurements in 3 WT mice transfused with the TRPC6-KO RBCs. We detected an increase in the Ca²⁺ response, as outlined in Figure 1C (dark red symbols). The slope of the regression line significantly differed from zero ($P < .0001$), indicating a real increase in the Ca²⁺ response. However, because PKH26 is a membrane-bound dye, we wanted to ensure that this result was not compromised by movement of the dye moving from the KO to the WT RBCs. Therefore, we crossbred the TRPC6-KO mouse with a mouse with red fluorescent erythrocytes in which the tdRFP is cytoplasmic.¹⁹ We repeated the experiments with 4 of these mice and obtained the same results as for the PKH26-labeled RBCs (Figure 1C, light red symbols). Because the slopes for the increase in Ca²⁺ were not significantly different upon PKH26 and tdRFP labeling, for all following considerations, we

pooled these 7 mice into a single statistical group. Figure 1D shows a statistical analysis comparing TRPC6-KO RBCs before transfusion (day 0) with RBCs 3 days and 10 days after transfusion with the response of WT RBCs. On day 3, the Ca²⁺ response was already significantly different compared with that of the nontransfused KO RBCs, and after 10 days, there was no difference between the transfused TRPC6-KO RBCs and WT cells. This result showed functional “rescue” (Ca²⁺ influx) of the TRPC6-KO cells, suggesting the uptake of TRPC6 from an external source in the KO RBCs. Regarding the mechanism of this protein transfer, we wondered about the role of the spleen, where RBCs experience strong mechanical interaction while passing through the interendothelial slits. Therefore, we repeated the transfusion experiments with splenectomized acceptor mice. The slope of the line representing Ca²⁺ entry again significantly differed from 0 ($P < .0001$) but also significantly differed from that obtained in the nonsplenectomized mouse experiments ($P < .001$), as shown in Figure 1E. Moreover, statistical analysis of the data from particular days pointed to a slower putative protein transfer process (Figure 1F). While on day 3, there was still no difference compared with the data collected upon TRPC6-KO before transfusion, it took 14 days until the transfused cells showed no difference from the WT RBCs.

The physiological function of TRPC6 in RBCs remained unknown, as was the case for other cation channels, such as the Gárdos channel or Piezo1, when they were discovered.⁶ The association of ion channel mutations to hematological diseases helped elucidate channel functions. We expect the same for TRPC6. Reports of mechanosensitivity of TRPC6²⁰ indicate some redundancy with Piezo1 or TRPV2 in RBC volume regulation.²¹ Furthermore, because TRPC6 is downstream of LPA-receptor activation,¹² it likely contributes to the active participation of RBCs in clot and thrombus formation,²² including pathological situations such as vaso-occlusive crisis in patients with sickle cell disease.¹²

Inspired by the mechanical challenge RBCs experience in the spleen, we applied forces up to 400 pN to pairs of human RBCs with the cantilever of an AFM²³ as schematically outlined in Figure 2A-B. Simultaneously, we performed confocal microscopy,²³ through which we witnessed the formation of membrane tethers (Figure 2C-D), structures that could mediate a protein exchange between cells. Even without the formation of tethers, the RBCs could strongly interact, as shown in Figure 2E-F. Furthermore, at a time scale that is too short to be imaged but more realistic to conditions in the spleen (millisecond range), atomic force spectroscopy revealed membrane binding effects in the range of 200 pN (Figure 2G), which is well above the adhesion forces between RBCs when attached to each other without the application of mechanical force.²⁴

Discussion

To date, the mechanism through which the protein transfer is mediated remains unknown. Identification of tether formation demonstrates the ability of RBCs to exchange/share membrane components. Whether protein transfer of TRPC6 to RBCs is an inter-RBC process, interaction with other cell types or with the exosome, remains elusive and requires further investigations.

The entire process is of great interest, especially because healthy RBCs under physiological conditions have not shown endocytic activity.²⁵ However, our observation is in line with previous findings

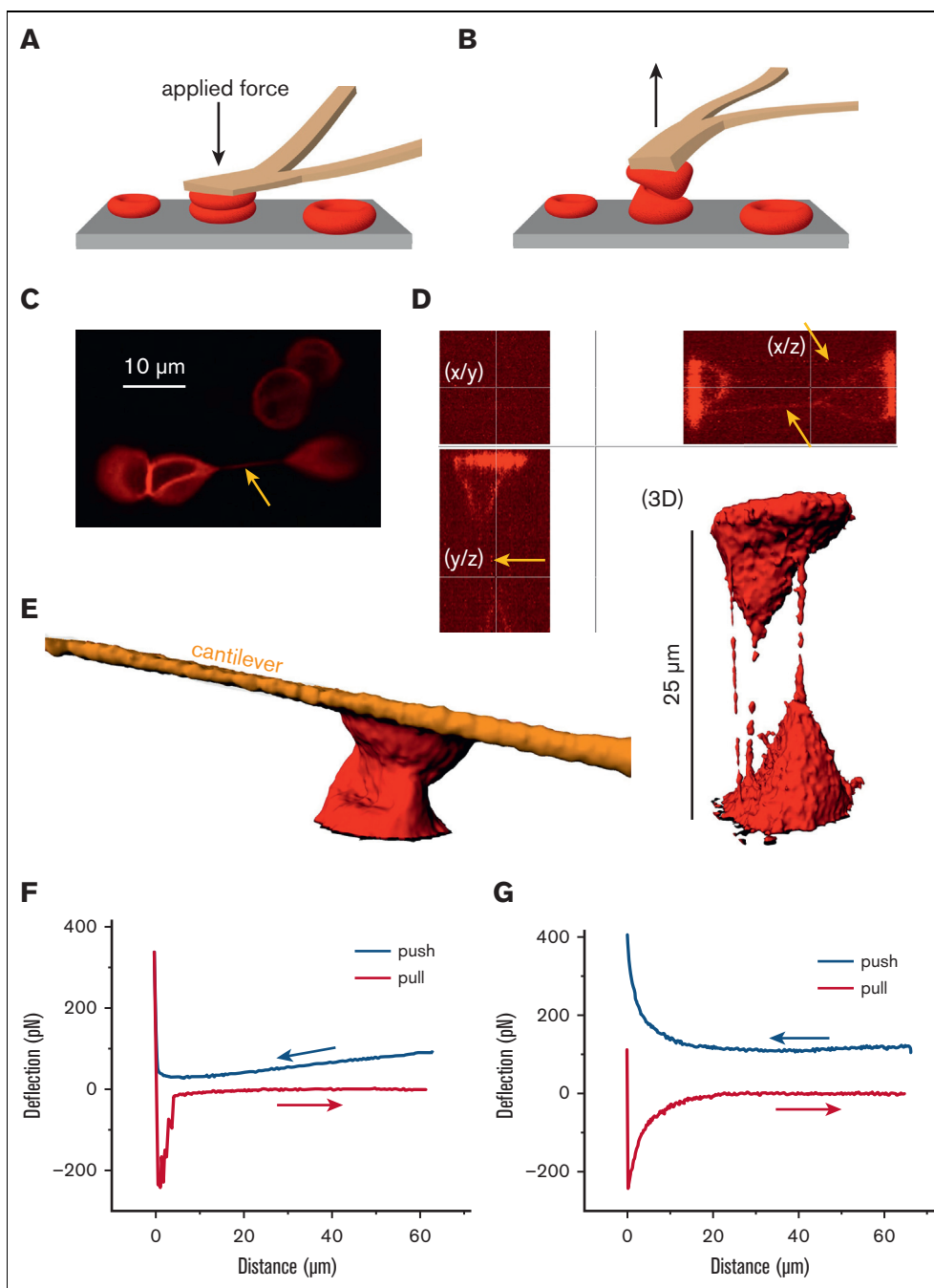


Figure 2. Mechanical challenge of human RBCs by atomic force spectroscopy. (A) Schematic drawing of the mechanical challenge owing to application of the cantilever of an AFM with forces of up to 400 pN applied. RBCs were attached to the cantilever with Cell-Tak (BD Biosciences, San Jose, CA) and spontaneously adhered to the microscope dish (microdish). (B) Schematic drawing showing the retraction of the cantilever with measurement of the separation force. (C) Confocal image of RBCs labeled with the membrane dye CellMask (Life Technologies, Carlsbad, CA) at 1:2000 for 10 minutes. The yellow arrow points to a tether, clearly connecting 2 RBCs. Scale bar, 10 μm . (D) Two RBCs were pushed together and separated, as outlined in panels A and B, in a plasma-like solution containing 40 mg/mL dextran (70 kDa). Shown are optical sections and the 3D reconstruction with clearly visible tethers in the x/z and y/z planes (yellow arrows) but few visible tethers in the x/y plane. The 3D reconstruction, in addition to the optical sections, reveals uneven staining of the tethers, suggesting the presence of lipid rafts or other molecular agglomerations. It is of little importance whether the tethers form between RBCs or between an RBC and the substrate, as protein transfer could potentially also occur between RBCs and structures of the spleen. (E) Even without the formation of tethers, RBCs strongly interact, potentially allowing a protein transfer. (F) Atomic force spectroscopy measurement reflecting the situation imaged in panel E with an RBC interaction time of several seconds. (G) Representative atomic force spectroscopy measurement with a contact time close to 0 and a velocity of the cantilever movement of 5 $\mu\text{m/s}$ in a dextran solution (40 mg/mL dextran 70 kDa) used to mimic plasma. Such a probing is too fast to be imaged by confocal microscopy.

regarding the transfer of band 3 protein from RBCs to vesicles and vice versa.²⁶ Furthermore, protein transfer to lymphocytes is well known and referred to as trogocytosis.²⁷

Conclusions

Although TRPC6 activity was indirectly probed and the in vitro experiments applied mechanical force, we regard our data as strong evidence for a new and thus far overlooked mechanism, with great potential for human medicine in general and hereditary diseases involving RBCs in particular. This holds especially true if the abundance (copy number) of the malfunctional protein of interest is very low, such as Piezo1 in hereditary xerocytosis²⁸ and KCNN4 in Gárdos channelopathy.^{3,29} However, for clinical applications, this effect would need to be further investigated and stimulated to reach a decent effect size.

Acknowledgments

The authors thank Petra Weißgerber for assistance with breeding and crossing the mouse lines, Sabrina Hennig for assistance in handling the mice, and Peter Lipp for the use of the fluorescence imaging setup.

This study was supported by grants from the European Framework Horizon 2020 (grant agreement number 860436

[EVIDENCE]), the Deutsche Forschungsgemeinschaft (German Research Foundation, grant number WA 1336/13-1) (C.W.), and in part by the intramural Research Program of the National Institutes of Health, Cell Signalling (Project Z01-ES-101684) (L.B.).

Authorship

Contribution: L.K. designed the study; L.B., C.W., and M.W.L. provided resources; L.K. and C.W. supervised the experiments; L.H. and D.F. performed and analyzed the experiments; M.W.L. performed the mouse surgery; L.B. organized the transcriptome analysis; L.K. drafted the manuscript; and all authors revised and approved the manuscript.

Conflict-of-interest disclosure: The authors declare no competing financial interests.

ORCID profiles: D.F., [0000-0003-0869-6850](https://orcid.org/0000-0003-0869-6850); L.B., [0000-0002-0775-8661](https://orcid.org/0000-0002-0775-8661); C.W., [0000-0001-7788-4594](https://orcid.org/0000-0001-7788-4594); M.W.L., [0000-0002-7847-8456](https://orcid.org/0000-0002-7847-8456); L.K., [0000-0001-6796-9535](https://orcid.org/0000-0001-6796-9535).

Correspondence: Lars Kaestner, Theoretical Medicine and Biosciences, Medical Faculty, Saarland University, Campus University Hospital, Building 61.4, 66421 Homburg, Germany; email: lars_kaestner@me.com.

References

1. Karsten E, Herbert BR. The emerging role of red blood cells in cytokine signalling and modulating immune cells. *Blood Rev.* 2020;41:100644.
2. Wagner-Britz L, Wang J, Kaestner L, Bernhardt I. Protein kinase C_{α} and P-type Ca channel $Ca_v2.1$ in red blood cell calcium signalling. *Cell Physiol Biochem.* 2013;31(6):883-891.
3. Jansen J, Qiao M, Hertz L, et al. Mechanistic ion channel interactions in red cells of patients with Gárdos channelopathy. *Blood Adv.* 2021;5(17):3303-3308.
4. Wang J, Wagner-Britz L, Bogdanova A, et al. Morphologically homogeneous red blood cells present a heterogeneous response to hormonal stimulation. *PLoS One.* 2013;8(6):e67697.
5. Bogdanova A, Kaestner L, Simionato G, Wickrema A, Makhro A. Heterogeneity of red blood cells: causes and consequences. *Front Physiol.* 2020;11:392.
6. Kaestner L, Bogdanova A, Egee S. Calcium channels and calcium-regulated channels in human red blood cells. *Adv Exp Med Biol.* 2020;1131:625-648.
7. Lindern M von, Egée S, Bianchi P, Kaestner L. The function of ion channels and membrane potential in red blood cells: toward a systematic analysis of the erythroid channelome. *Front Physiol.* 2022;13:824478.
8. Grygorczyk R, Schwarz W, Passow H. Ca^{2+} -activated K^+ channels in human red cells. Comparison of single-channel currents with ion fluxes. *Biophys J.* 1984;45(4):693-698.
9. Egée S, Lapaix F, Decherf G, et al. A stretch-activated anion channel is up-regulated by the malaria parasite *Plasmodium falciparum*. *J Physiol.* 2002;542(Pt 3):795-801.
10. Kaestner L. Channelizing the red blood cell: molecular biology competes with patch-clamp. *Front Mol Biosci.* 2015;2:46.
11. Foller M, Kasinathan RS, Koka S, et al. TRPC6 contributes to the $Ca(2+)$ leak of human erythrocytes. *Cell Physiol Biochem.* 2008;21(1-3):183-192.
12. Wang J, Hertz L, Ruppenthal S, et al. Lysophosphatidic acid-activated calcium signaling is elevated in red cells from sickle cell disease patients. *Cells.* 2021;10(2):456.
13. Kaestner L, Minetti G. The potential of erythrocytes as cellular aging models. *Cell Death Differ.* 2017;24(9):1475-1477.
14. Danielczok J, Hertz L, Ruppenthal S, et al. Does erythropoietin regulate TRPC channels in red blood cells? *Cell Physiol Biochem.* 2017;41(3):1219-1228.
15. Beutler E, West C, Blume KG. The removal of leukocytes and platelets from whole blood. *J Lab Clin Med.* 1976;88(2):328-333.
16. Achilli C, Ciana A, Balduini C, Risso A, Minetti G. Application of gelatin zymography for evaluating low levels of contaminating neutrophils in red blood cell samples. *Anal Biochem.* 2011;409(2):296-297.

17. Kaestner L, Tabellion W, Weiss E, Bernhardt I, Lipp P. Calcium imaging of individual erythrocytes: problems and approaches. *Cell Calcium*. 2006;39(1):13-19.
18. Belkacemi A, Trost CF, Tinschert R, et al. The TRPV2 channel mediates Ca²⁺ influx and the Δ9-THC-dependent decrease in osmotic fragility in red blood cells. *Haematologica*. 2021;106(8):2246-2250.
19. Hertz L, Ruppenthal S, Simionato G, et al. The evolution of erythrocytes becoming red in respect to fluorescence. *Front Physiol*. 2019;10:753.
20. Spassova MA, Hewavitharana T, Xu W, Soboloff J, Gill DL. A common mechanism underlies stretch activation and receptor activation of TRPC6 channels. *Proc Natl Acad Sci U S A*. 2006;103(44):16586-16591.
21. Egee S, Kaestner L. The transient receptor potential vanilloid type 2 (TRPV2) channel - a new druggable Ca²⁺ pathway in red cells, implications for red cell ion homeostasis. *Front Physiol*. 2021;12:677573.
22. Bernhardt I, Wesseling MC, Nguyen DB, Kaestner L. Red blood cells actively contribute to blood coagulation and thrombus formation. *Erythrocyte*. 2019.
23. Abay A, Simionato G, Chachanidze R, et al. Glutaraldehyde - a subtle tool in the investigation of healthy and pathologic red blood cells. *Front Physiol*. 2019;10:514.
24. Minetti G, Egée S, Mörsdorf D, et al. Red cell investigations: art and artefacts. *Blood Rev*. 2013;27(2):91-101.
25. Gao X, Yue T, Tian F, Liu Z, Zhang X. Erythrocyte membrane skeleton inhibits nanoparticle endocytosis. *AIP Adv*. 2017;7(6):065303.
26. Newton AC, Cook SL, Huestis WH. Transfer of band 3, the erythrocyte anion transporter, between phospholipid vesicles and cells. *Biochemistry*. 1983;22(26):6110-6117.
27. Dance A. Core Concept: cells nibble one another via the under-appreciated process of trogocytosis. *Proc Natl Acad Sci U S A*. 2019;116(36):17608-17610.
28. Zarychanski R, Schulz VP, Houston BL, et al. Mutations in the mechanotransduction protein PIEZO1 are associated with hereditary xerocytosis. *Blood*. 2012;120(9):1908-1915.
29. Fermo E, Bogdanova A, Petkova-Kirova P, et al. "Gardos channelopathy": a variant of hereditary stomatocytosis with complex molecular regulation. *Sci Rep*. 2017;7(1):1744.